Chemical Looping Methanol Oxidation using Supported Vanadium Phosphorous Oxide Carriers for Formaldehyde Production

*Anuj S. Joshi ‡ [a], Sonu Kumar ‡ [a], Melissa Marx [b], Amanda H. Trout [c], Sudeshna Gun [a], Zain Mohammad [a], Yehia Khalifa [b], Liang-Shih Fan * [a]*

[a] William G. Lowrie Department of Chemical and Biomolecular Engineering, The Ohio State University, 151 West Woodruff Avenue, Columbus, OH 43210, USA

[b] Department of Chemistry and Biochemistry, The Ohio State University, 151 West Woodruff Avenue, Columbus, OH 43210, USA

[c] Center for Electron Microscopy and Analysis, Department of Materials Science and Engineering, The Ohio State University, 1305 Kinnear Rd., Columbus, OH 43212, USA

‡ These authors have contributed equally to this work.

* Corresponding author. *Email address*: fan.1@osu.edu (L.-S. Fan)

Supplementary Information

S1. Fixed Bed Reactor Setup

Figure S1 depicts the fixed bed reactor setup.

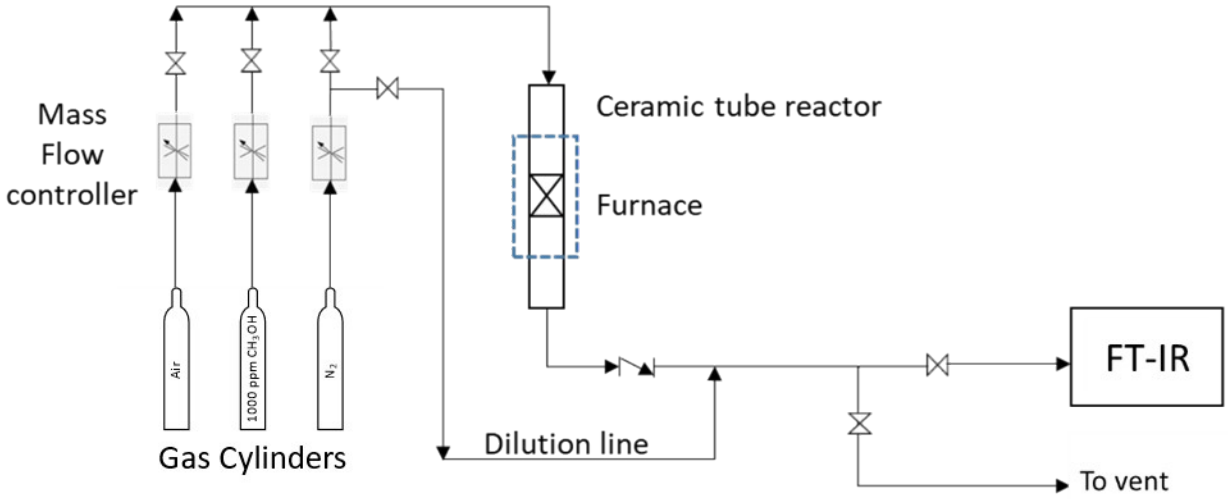

Figure S1: Fixed bed reactor setup

S2. N_2 Adsorption-Desorption Isotherms for calcined-SiO_2

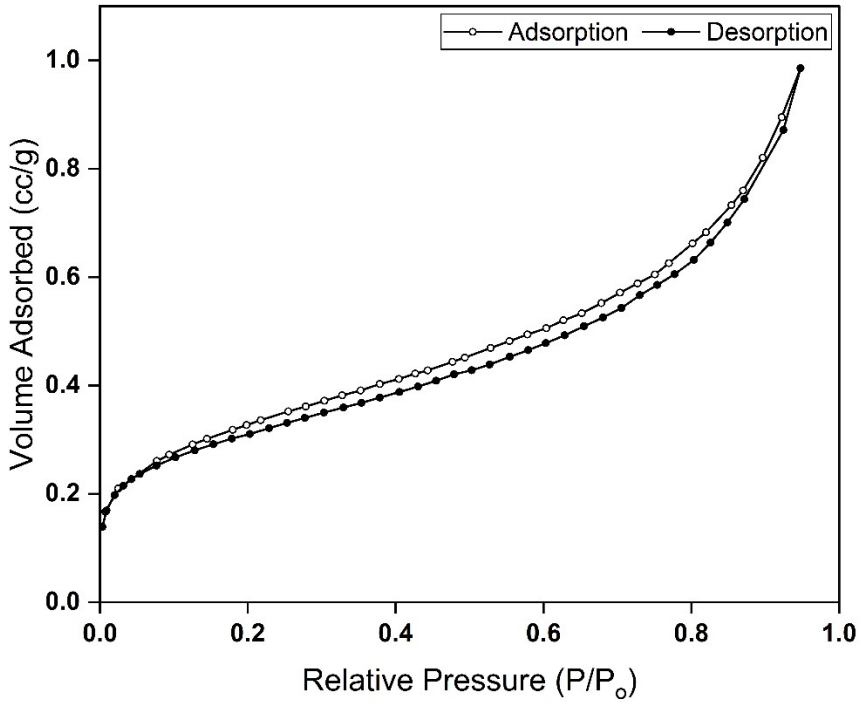

Figure S2: N_2 Adsorption-Desorption Isotherms for calcined-SiO_2

S3. Fresh and Post 10 Redox XRD analysis of VPO-30Si and VPO-50Si

The XRD spectra of the fresh VPO-30Si and VPO-50Si are shown in Figure S3. The spectra indicate that VPO-30Si and VPO-50Si were synthesized successfully and maintained their phase integrity over 10 redox cycles.

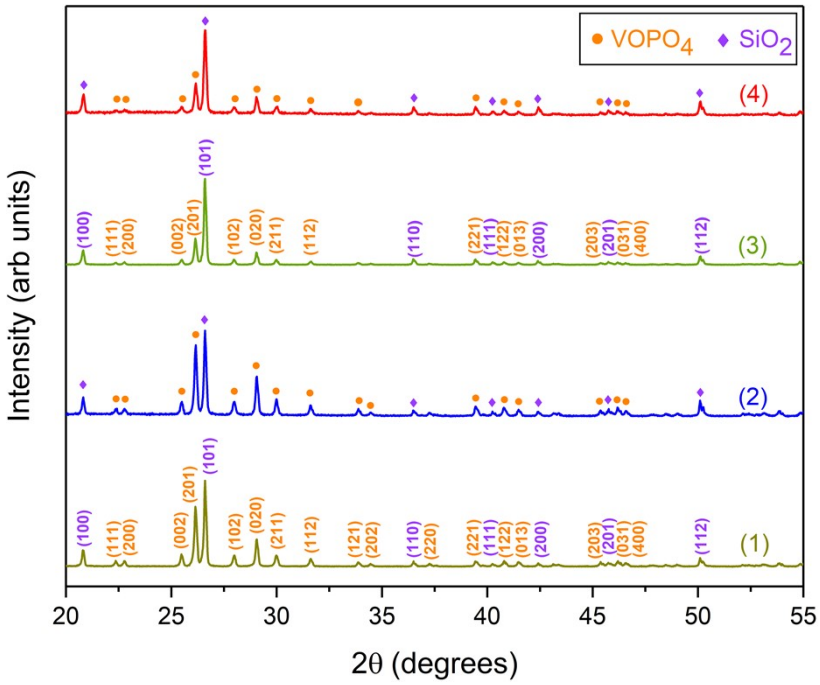

Figure S3: XRD spectra of VPO-30Si (a) before and (2) after 10 redox cycles and of VPO-50Si (3) before and (4) after 10 redox cycles

S4. Fresh and After 10 Redox XPS analysis of VPO-Un and VPO-70 Si

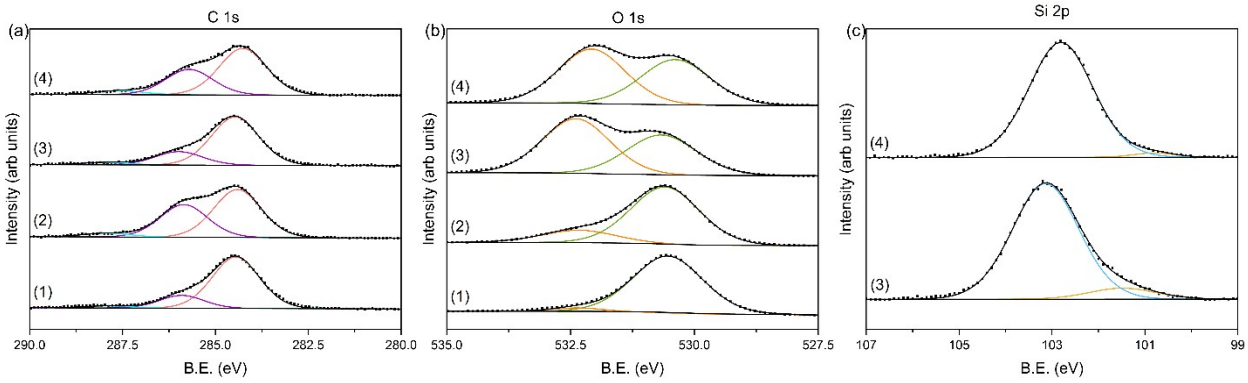

Figure S4: (a) C 1s XPS spectra (b) O 1s XPS spectra and (c) Si 2p XPS spectra of VPO-Un (1) before and (2) after 10 redox cycles and of VPO-70Si (3) before and (4) after 10 redox cycles

For the C 1s region, as shown in Figure S4(a), the aliphatic carbon feature (284.5 eV), a C-O feature (285.7 eV), as well as a weak feature at (287.6 eV), which has been previously cited as being C=O are observed.[1–3] These features appear in all samples regardless of if they are supported or unsupported, or cycled.

In the O 1s region, as shown in Figure S4(b), the VPO-Un carriers show two different features. At 530.5 eV, there is the O-V^{+5} feature, as well as a weak feature at 532.4 eV. For the VPO-70Si carrier, there is a significant peak at 532.0 eV. This peak represents SiO_2, as seen in the literature. The constant feature in the O 1s (530.4 eV), regardless of supported/unsupported or cycled/uncycled, is again believed to be representative of the O-V^{+5}.[4]

For the Si 2p region, as shown in Figure S4(c), there is the major feature (SiO_2) at 103.1 eV, which slightly shifts to a lower binding energy of 102.8 eV after 10 redox cycles. This shift could be due to the varying oxygen component of SiO_x.[5] The other weak feature that is present in the Si 2p (101.5 eV) is consistent with that of a SiO species.[5]

S5. After 1 Redox XPS analysis of VPO-Un and VPO-70 Si

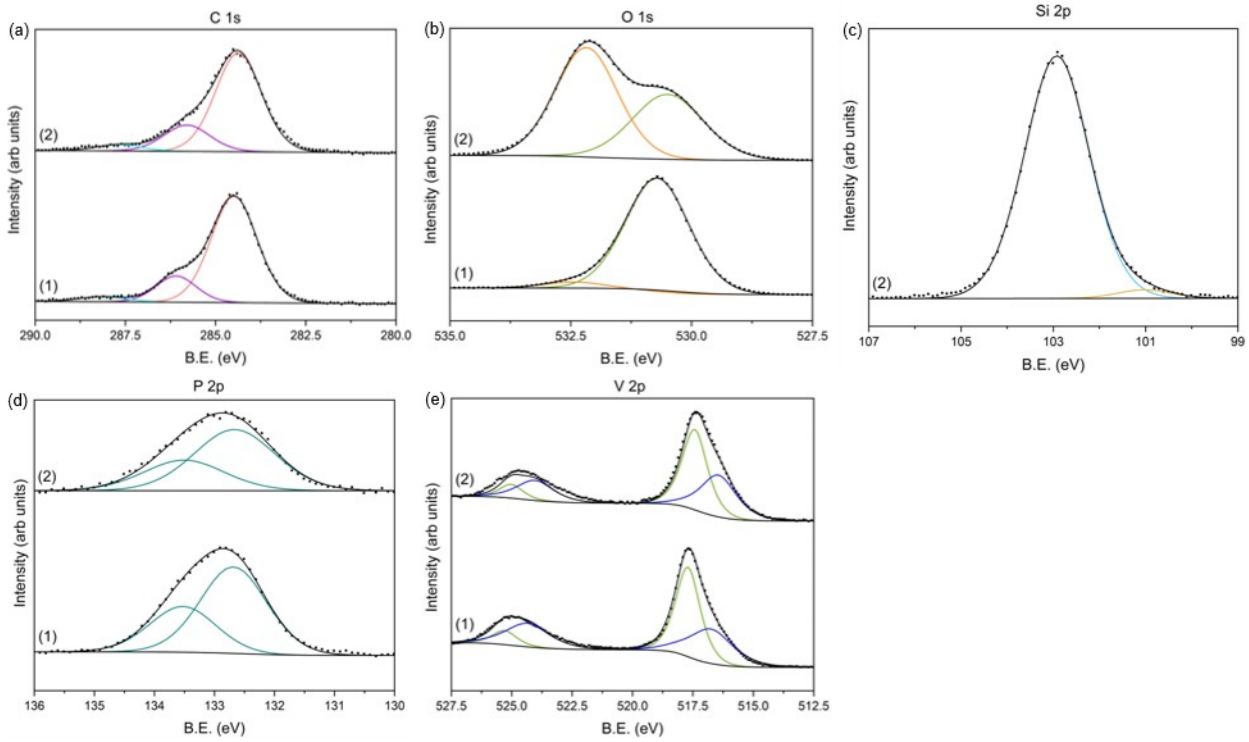

Figure S5: (a) C 1s XPS spectra (b) O 1s XPS spectra (c) Si 2p XPS spectra (d) P 2p XPS spectra and (e) V 2p XPS spectra after 1 redox cycle of (1) VPO-Un and (2) VPO-70Si

Figure S5(a) depicts the comparison of the C 1s region for the post 1 redox VPO-Un and VPO-70Si carriers. Here, three features can be seen at 284.5 eV (aliphatic carbon), 286.1 eV (C-O), and 288.1 eV (C=O) for both carriers. For the O 1s spectra, as shown in Figure S5(b), there is a clear difference between the unsupported and supported samples. The VPO-Un carrier has a large component at 530.7 eV ($O\text{-}V^{+5}$) and a weak feature at 532.4 eV. The VPO-70Si carrier, on the other hand, has two distinct oxygen features at 530.4 eV ($O\text{-}V^{+5}$) and 532.2 eV. Given that the support is SiO_2, it can be concluded that the larger (532.2 eV) of these represents the Si-O bond. The Si 2p spectrum, shown in Figure S5(c), is very similar to that seen in Figure S4(c), with a larger feature at 103.0 eV (SiO_2) and a weaker feature at 101.0 eV (SiO). P 2p spectra, depicted in Figure S5(d), indicate similar spectral components for both the supported and unsupported carriers. Features at 132.7 eV and 133.5 eV represent the P $2p_{3/2}$ and P $2p_{1/2}$, respectively. V 2p spectra are illustrated in Figure S5(e) and show similar features as discussed in the main text. Two sets of doublets (V $2p_{3/2}$ and V $2p_{1/2}$) that are representative of both the V^{+5} (517.6 eV and 525.2 eV) and the V^{+4} (516.6 eV and 524.2 eV) state are observed.

S6. Energy Dispersive X-ray Spectroscopy on Fresh and Post-10 Redox VPO-Un and VPO-70Si carriers

The SEM images, along with corresponding EDS elemental mapping for both the fresh and post-redox carriers, are depicted below in Figures S6-S9.

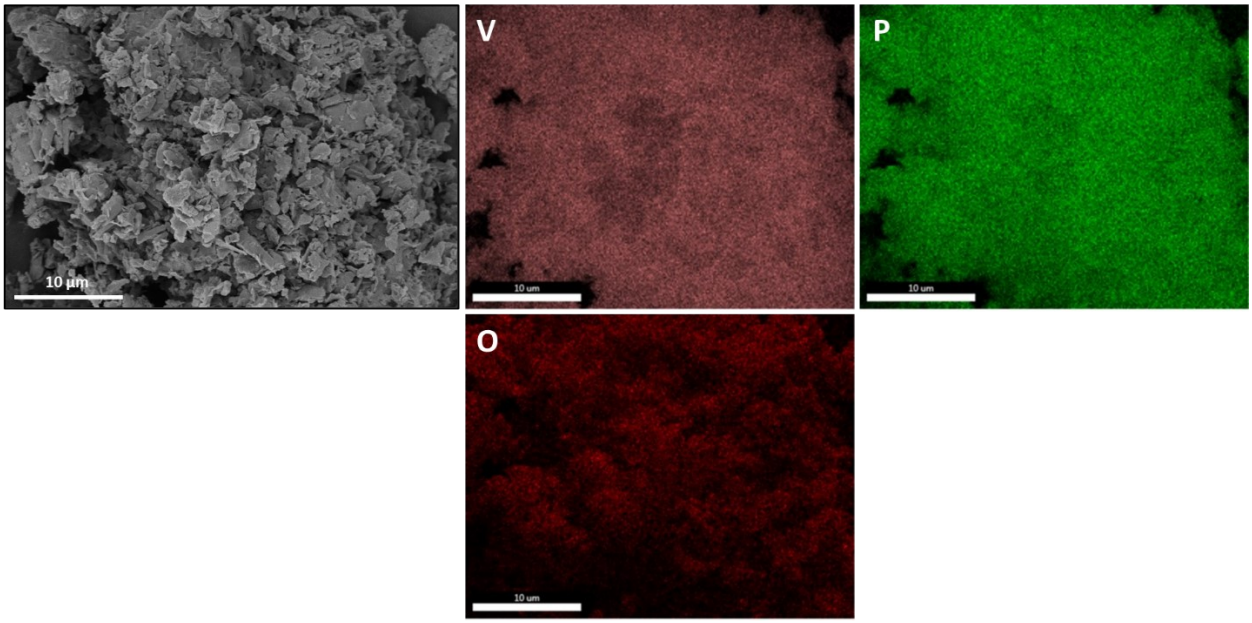

Figure S6: SEM image and EDS mapping of V, P, and O of fresh VPO-Un carrier

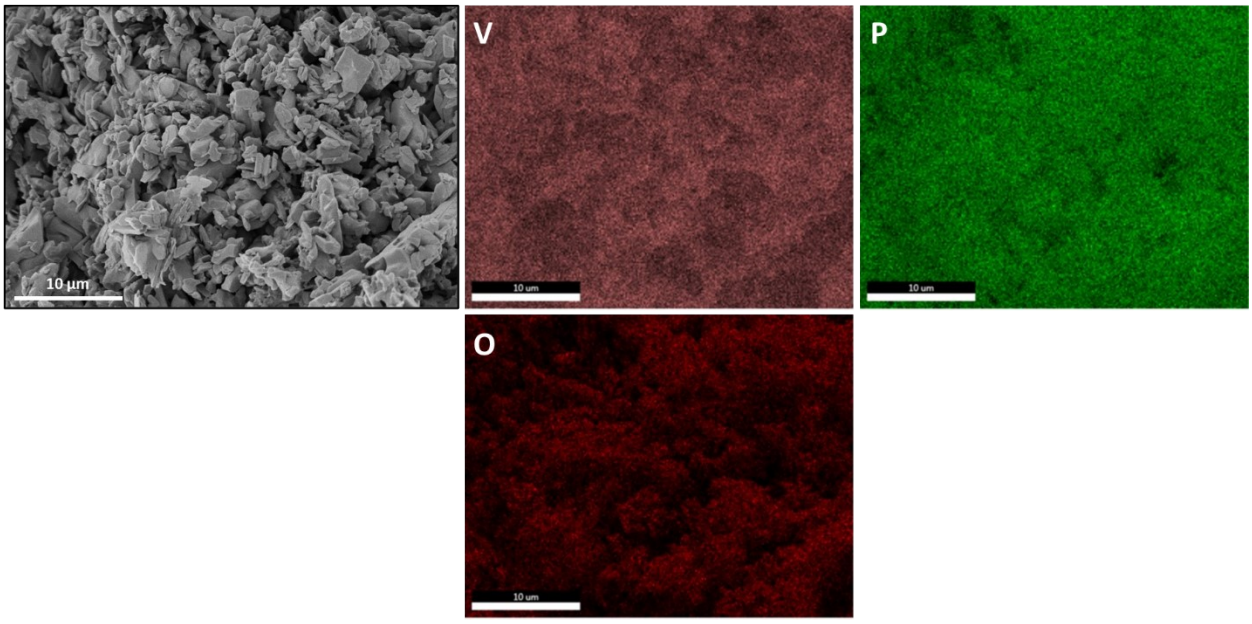

Figure S7: SEM image and EDS mapping of V, P, and O of after 10 redox VPO-Un carrier

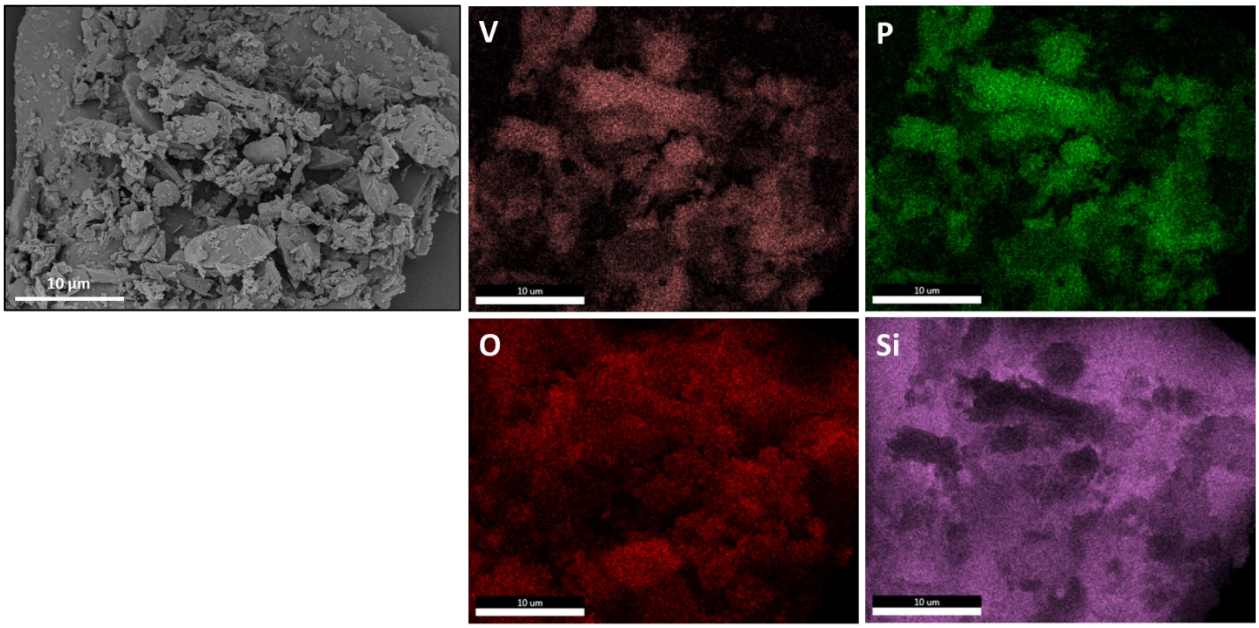

Figure S8: SEM image and EDS mapping of V, P, O, and Si of fresh VPO-70Si carrier

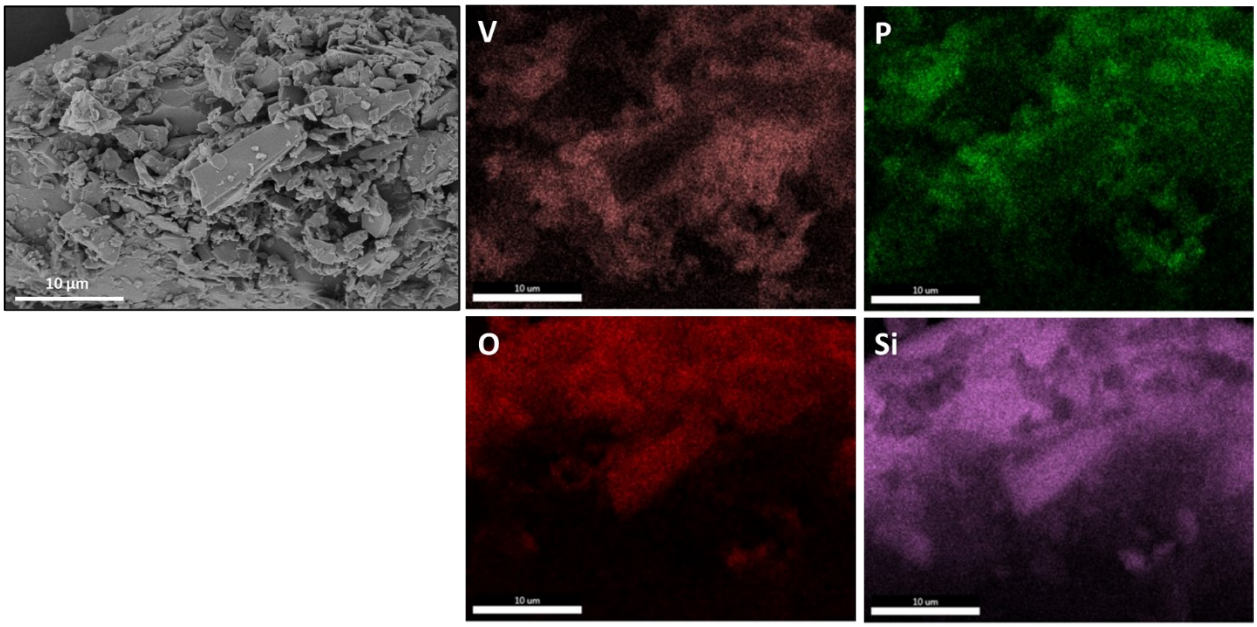

Figure S9: SEM image and EDS mapping of V, P, O, and Si of after 10 redox VPO-70Si carrier

S7. Characterization of VPO-Un carrier post 3-hour CH_3OH reduction

Figure S10 represents the XRD spectra after air oxidation following the 3-hour reduction under CH_3OH. It can be seen from the spectra that complete regeneration to the $VOPO_4$ phase is obtained.

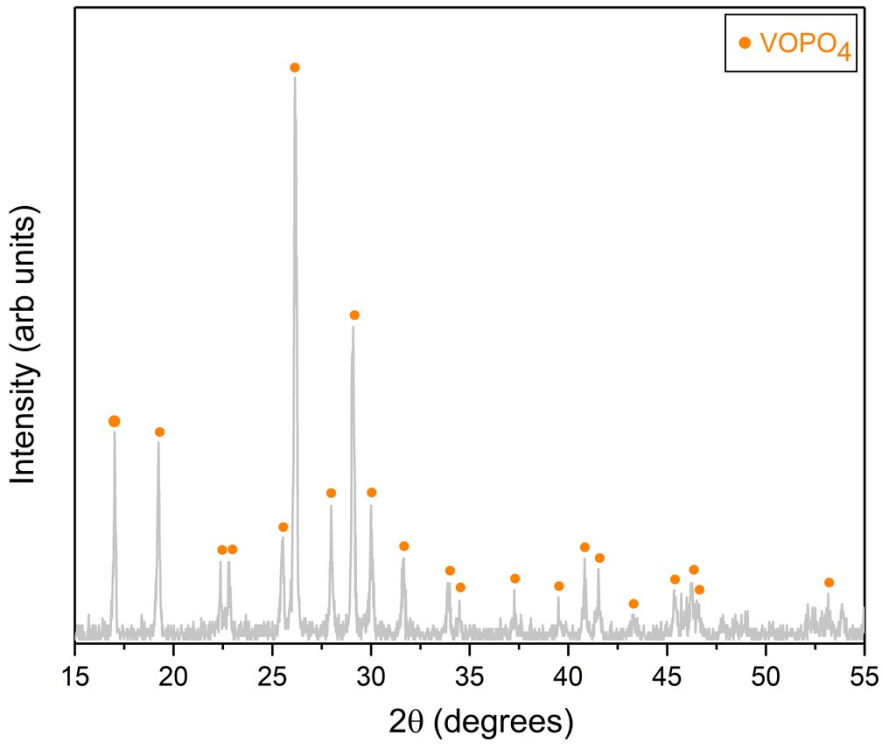

Figure S10: XRD spectrum of regenerated VPO-Un after 3-hour CH_3OH reduction

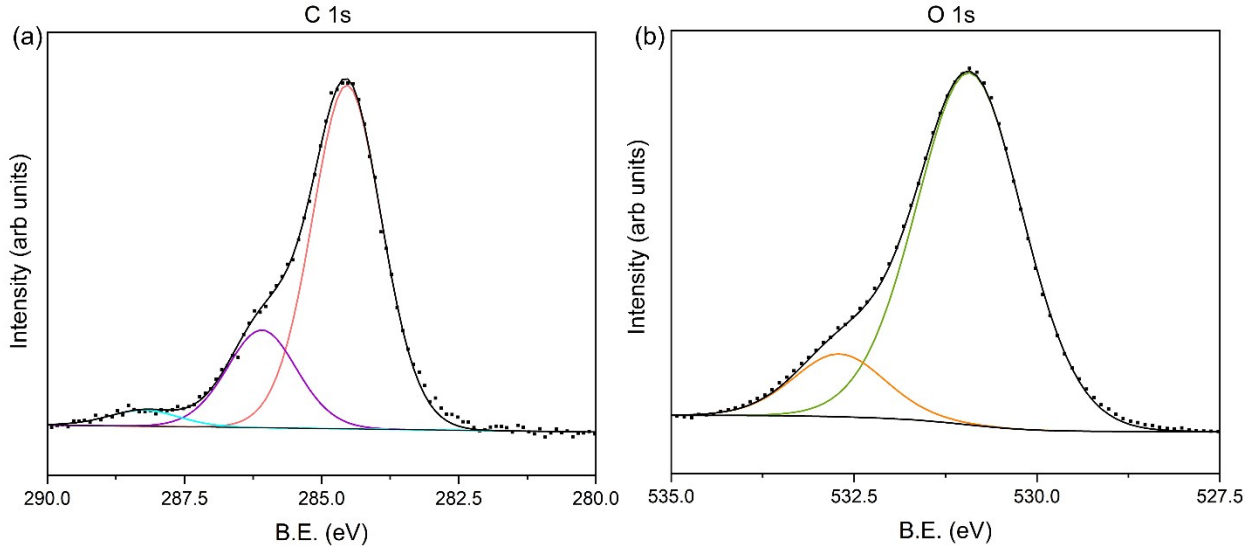

Figure S11: (a) C 1s XPS spectra and (b) O 1s XPS spectra of VPO-Un after 3 hours CH3OH reduction

XPS spectrum of post 3 hours CH_3OH on VPO undoped for both the C 1s region and the O 1s region is shown in Figure S11(a) and S11(b), respectively. The C 1s region has three distinct features at 284.5 eV (aliphatic carbon), 286.1 eV (C-O), and 288.2 eV (C=O). The O 1s region only has two spectral components at 530.9 eV (O-V^{5+}) and 532.7 eV (OH). [1–4]

S8. Redox analysis on carriers

The oxygen loss calculated based on TGA weight reduction data for all four carriers is presented in Figure S12.

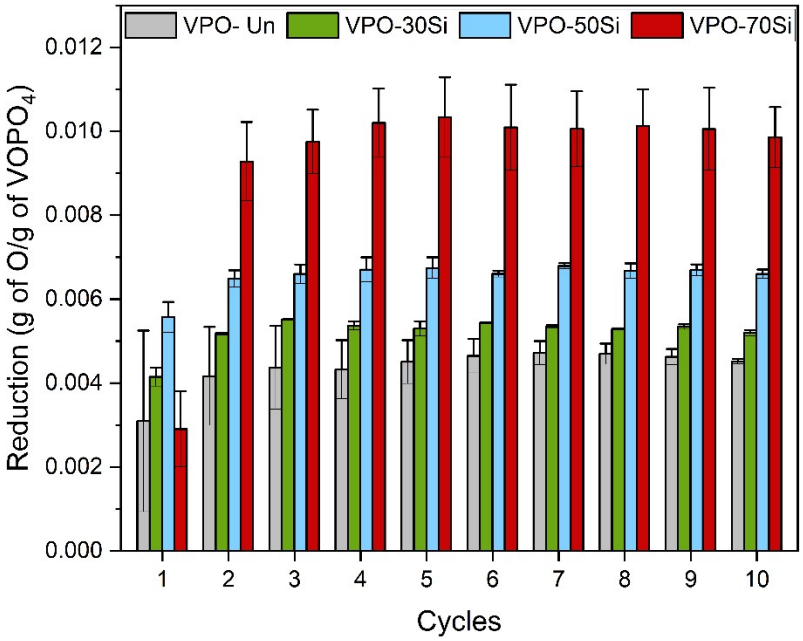

Figure S12: Oxygen loss of VPO-Un, VPO-30Si, VPO-50Si, and VPO-70Si carriers across 10 redox cycles

S9. Fixed Bed Analysis

The outlet gas concentration profile for the VPO-70Si fixed bed experiment is provided in Figure S13.

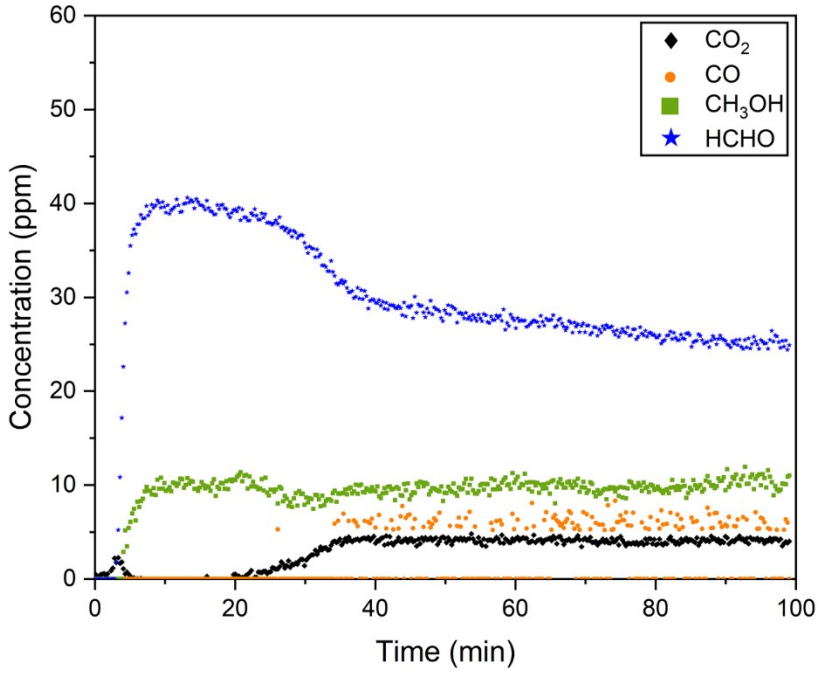

Figure S13: Outlet gas concentration profile of VPO-70Si in fixed bed (post dilution)

The fixed bed experiment analysis for the VPO-Un carrier, along with the corresponding outlet gas concentration profile, is depicted in Figure S14.

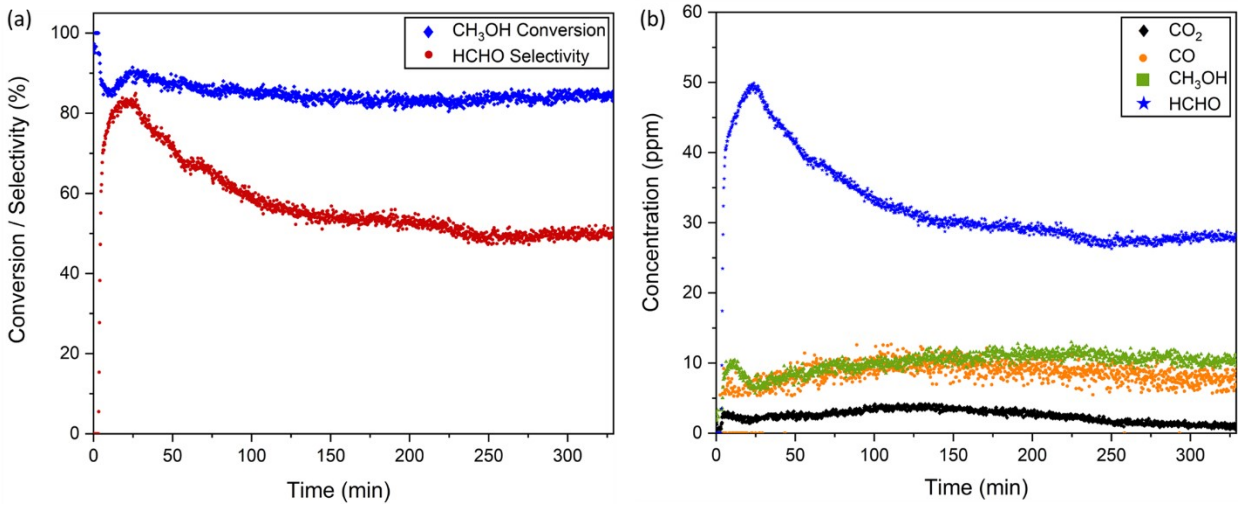

Figure S14: (a) CH_3OH conversion and HCHO selectivity and (b) Outlet gas concentration profile of VPO-Un in fixed bed

The recorded IR spectrum of the reactor outlet gas stream at different time intervals during the VPO-70Si fixed bed experiment is presented in Figure S15.

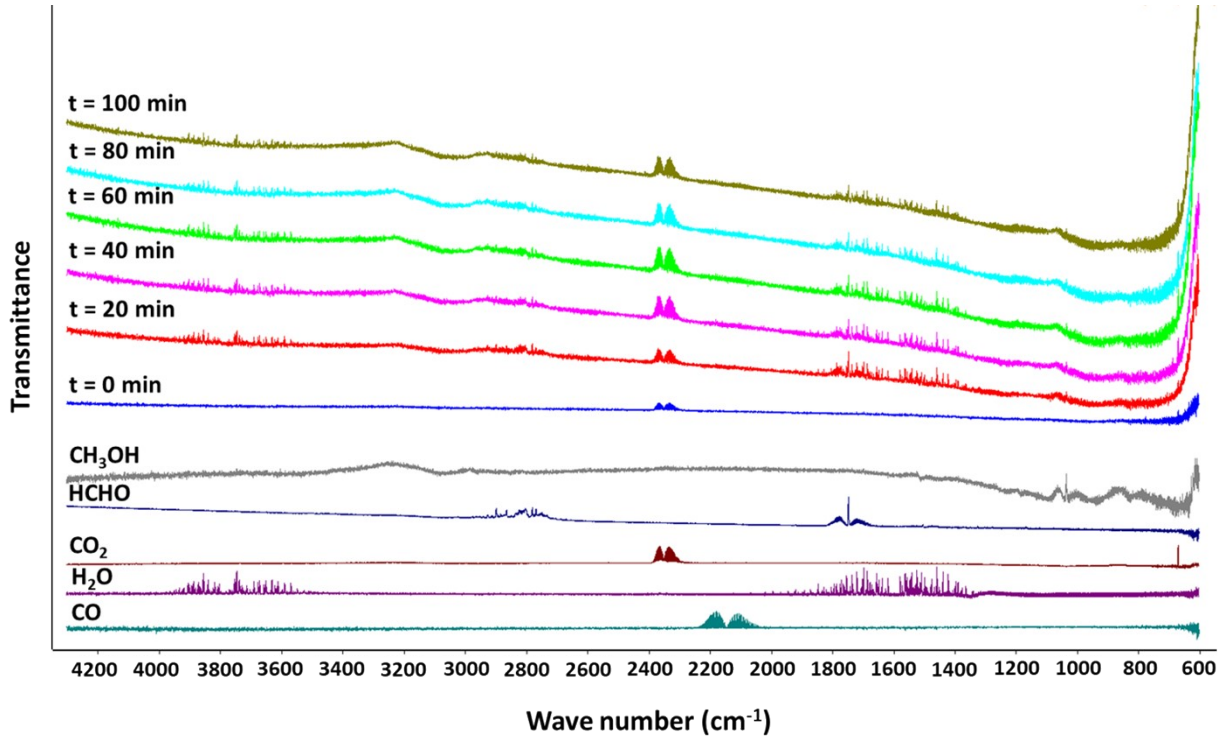

Figure S15: IR spectra of outlet gases in fixed bed for VPO-70Si at different time intervals along with pure components

The TGA curves of the VPO-Un carrier, depicting weight versus time for different periods of reduction under CH_3OH, are depicted in Figure S16.

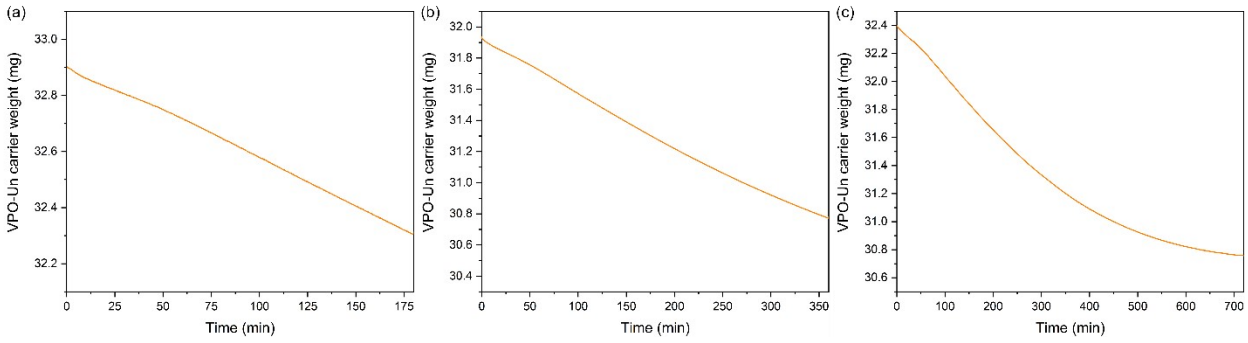

Figure S16: TGA curves of CH_3OH reduction of VPO-Un at 400°C for (a) 3 hours (b) 6 hours and (c) 12 hours

References

(1) X. Chen, X. Wang, D. Fang, A review on C1s XPS-spectra for some kinds of carbon materials, Fullerenes, Nanotubes and Carbon Nanostructures. 28 (2020) 1048–1058.

(2) S. Gull, S.-C. Huang, C.-S. Ni, S.-F. Liu, W.-H. Lin, H.-Y. Chen, Operando synchrotron X-ray studies of MnVOH@ SWCNT nanocomposites as cathodes for high-performance aqueous zinc-ion batteries, Journal of Materials Chemistry A. 10 (2022) 14540–14554.

(3) R.B. Ambade, S.B. Ambade, R.S. Mane, S.-H. Lee, Interfacial engineering importance of bilayered ZnO cathode buffer on the photovoltaic performance of inverted organic solar cells, ACS Applied Materials & Interfaces. 7 (2015) 7951–7960.

(4) M. Nadolska, M. Szkoda, K. Trzciński, P. Niedziałkowski, J. Ryl, A. Mielewczyk-Gryń, K. Górnicka, M. Prześniak-Welenc, Insight into Potassium Vanadates as Visible-Light-Driven Photocatalysts: Synthesis of V(IV)-Rich Nano/Microstructures for the Photodegradation of Methylene Blue, Inorg. Chem. 61 (2022) 9433–9444. https://doi.org/10.1021/acs.inorgchem.2c00136.

(5) R. Alfonsetti, L. Lozzi, M. Passacantando, P. Picozzi, S. Santucci, XPS studies on SiO_x thin films, Applied Surface Science. 70 (1993) 222–225.